The Plant Cell, Vol. 15, 331–345, February 2003, www.plantcell.org © 2003 American Society of Plant Biologists

Regulation of Actin-Dependent Cytoplasmic Motility by Type II Phytochrome Occurs within Seconds in *Vallisneria gigantea* Epidermal Cells

Shingo Takagi,[a,1] Sam-Geun Kong,[b,2] Yoshinobu Mineyuki,[c] and Masaki Furuya[b]

[a] Department of Biology, Graduate School of Science, Osaka University, Toyonaka, Osaka 560-0043, Japan
[b] Hitachi Advanced Research Laboratory, Hatoyama, Saitama 350-0395, Japan
[c] Department of Biological Science, Graduate School of Science, Hiroshima University, Higashi-Hiroshima, Hiroshima 739-8526, Japan

The effects of light on actin-dependent cytoplasmic motility in epidermal cells of green leaves of the aquatic angiosperm *Vallisneria gigantea* were investigated quantitatively using a custom-made dynamic image analyzer. Cytoplasmic motility was measured by monitoring changes in the brightness of individual pixels on digitized images taken sequentially under infrared light. Acceleration and deceleration of cytoplasmic motility were regulated photoreversibly by type II phytochrome(s). This phytochrome-dependent induction of cytoplasmic motility did not occur uniformly in cytoplasm but took place as scattered patches in which no particular organelles, including nucleus, existed. The induction became detectable at 2.5 s after the start of irradiation with pulsed red light. In cells exposed to microbeam irradiation, cytoplasmic motility was induced only in sites in the cytoplasm that were irradiated directly, whereas nonirradiated neighboring areas were unaffected. The effect was short-lived, disappearing within a few minutes, and no signal was transmitted from an irradiated cell to its neighbors. Anti-phytochrome antibody–responsive protein(s) was detectable in the leaf extract by immunoblot and zinc blot analyses and in cryosections of the epidermis by immunocytochemistry. Although the phytochrome-dependent cytoplasmic motility was blocked by exogenously applied latrunculin B or cytochalasins, treatment of the dark-adapted cells with Ca^{2+}-chelating reagents induced the cytoplasmic motility. We have proposed a model for the phytochrome regulation of cytoplasmic motility as one of the earliest responses to a light stimulus.

INTRODUCTION

Cytoplasmic movement is a phenomenon that is ubiquitous throughout the plant kingdom, and different types of movement have been described in detail by Britz (1979), Gunning (1982), and Nagai (1993). In many cases, prominent cell organelles such as nucleus and plastids move either constitutively or in response to external stimuli together with a mobile cytoplasmic matrix. For active cytoplasmic movements to occur, the cytoplasm must have a high motility. A change in the mode of cytoplasmic motility was induced rapidly by light in a green alga (Schönbohm, 1972) and higher plants (Takagi and Nagai, 1985; Kagawa and Wada, 2000). Although the light-dependent regulation of cytoplasmic motility in plant cells has long been of interest, no quantitative analysis of this phenomenon has been reported. This is attributable mainly to the fact that movements occur so rapidly that they are unable to be dissected by conventional methods of light microscopy.

To address this problem, a digital image-processing technique was developed based on the temporal analysis of changes in the brightness of individual pixels on optical images (Mineyuki et al., 1983). This technique was applied to the study of dynamic changes in the pattern of organelle movement during the progression of the cell cycle in fern protonemata (Mineyuki et al., 1984). We also designed and constructed an infrared (IR) Nomarski microscope for the continuous observation of living cells without any influence of observing light, to which a digital image analyzer was connected for photon counting and dynamic image processing (Furuya and Inoue, 1994). This microscope was developed further to enable microbeam irradiation of target cells without interference from observing light. Using this instrument, Nick et al. (1993) reported phytochrome-induced, long-distance signaling from an irradiated single cell or cluster of cells to unirradiated regions in the cotyledon of white

[1] To whom correspondence should be addressed. E-mail shingot@bio.sci.osaka-u.ac.jp; fax 81-6-6850-5817.
[2] Current address: Department of Botany, Graduate School of Science, Kyoto University, Kyoto 606-8502, Japan.
Article, publication date, and citation information can be found at www.plantcell.org/cgi/doi/10.1105/tpc.007237.

mustard that influenced the pattern of expression of mRNA for chalcone synthase and the biosynthesis of anthocyanin. More recently, long-distance propagation of a type II phytochrome-induced, short-lived signal for the induction of mRNA expression of the chlorophyll *a/b* binding protein in tobacco cotyledons was shown using the same equipment (Bischoff et al., 1997; Schütz and Furuya, 2001).

The recent progress of molecular approaches to the study of phytochromes has resulted in an enormous increase in our knowledge of the structure-function relationship of phytochromes (Quail et al., 1995), the roles of each member of the phytochrome gene family, and downstream signaling (Neff et al., 2000). By contrast, little is known about the intracellular events that occur immediately after the absorption of light by phytochromes. In early studies, rapid effects of phytochrome on the pelletability of phytochrome (Quail et al., 1973), changes in bioelectric potentials (Jaffe, 1968), and enzymatic activities (Oelze-Karow and Mohr, 1973) were reported. However, no significant progress was made until the recent discovery that green fluorescent protein–fused phytochrome A (Kircher et al., 1999) and native phytochrome A (Hisada et al., 2000) translocate from the cytoplasm to the nucleus within a few minutes after red light irradiation. Considering the importance of early downstream responses of phytochromes, we investigated the photoregulation of cytoplasmic motility in epidermal cells of *Vallisneria gigantea* using the microscope described above equipped with an image analyzer and a microbeam irradiator. We selected this material because previous studies with Vallisneria have demonstrated light-regulated reorientation of chloroplasts under dim and strong light (Izutani et al., 1990; Dong et al., 1995), light-induced rotational streaming of the cytoplasm (Yamaguchi and Nagai, 1981), and light-induced reorganization of the actin cytoskeleton (Dong et al., 1998). In addition, extracts prepared from green leaves of Vallisneria contain phytochrome that undergoes spectrophotometrically red/far-red photoreversible changes in absorption (Takagi et al., 1990). Because the cytoplasmic movement described above occurs in the course of minutes, it has been suggested that light-dependent intracellular movements may provide a suitable model for investigations of the early processes of light signal transduction (Wada et al., 1993).

Phytochrome-regulated responses in plants have been classified into three categories based on fluence and/or wavelength dependence. These are the very-low-fluence responses, low-fluence red/far-red reversible responses (Shinomura et al., 1996), and high-irradiance reactions (Shinomura et al., 2000). In the past decade, the roles of individual members of the phytochrome gene family have been assigned successfully using null mutants for specific phytochromes and phytochrome signaling components, predominantly in Arabidopsis (Neff et al., 2000). However, in the case of Vallisneria, it is difficult to perform this kind of analysis, because the phytochrome gene family has not yet been characterized and no phytochrome-deficient mutants are available. Nevertheless, in several species, it has been possible to identify two pools of phytochrome that are physiologically, spectrophotometrically, and immunochemically distinct. These are termed type I and type II phytochromes and are defined operationally in terms of their light stability in vivo and their detection by specific monoclonal antibodies (Furuya, 1993). In the absence of detailed molecular information about the phytochrome family in Vallisneria, we have attempted to identify which phytochrome type (I or II) might be involved in the rapid light-induced cytoplasmic motility using a dynamic image-processing method. Here, we show that phytochrome induction of cytoplasmic motility occurs within seconds of light exposure and thus is one of the most rapid responses to type II phytochrome reported to date.

RESULTS

Quantitative Visualization of Cytoplasmic Motility

The newly developed image-processing method was applied to a quantitative analysis of cytoplasmic motility in epidermal cells of Vallisneria. After irradiation with white light of different intensities, samples determined visually to show low (Figure 1A), intermediate (Figure 1D), and high (Figure 1G) cytoplasmic motility were analyzed by the dynamic image-processing method. The equipment is illustrated schematically in Figure 1J. Each result was demonstrated in terms of the processed image in false color (Figures 1B, 1E, and 1H) and the frequency distribution of calculated indices for individual pixels (Figures 1C, 1F, and 1I). The peak values of the calculated indices of cytoplasmic motility for the low-, intermediate-, and high-motility samples were 13.5 (Figure 1C), 21.6 (Figure 1F), and 39.2 (Figure 1I), respectively. We concluded that this index can be used to provide a quantitative scale of cytoplasmic motility.

Using this method, the effects of dark adaptation and light irradiation on cytoplasmic motility were investigated. Sample leaves were exposed to white light for 12 h under the daily regime and then kept in complete darkness for various periods of time. During a 12-h dark incubation, the cytoplasmic motility index decreased gradually from $>$20 to 14. Upon white light illumination of the dark-adapted samples, numerous clusters of bright pixels appeared as scattered patches in the cytoplasm facing the outer periclinal wall of the epidermal cells (Figure 2). The number and size of bright clusters depended on the fluence of the incident light. The site of these areas of cytoplasmic movement did not correspond to any particular visible organelles, such as nuclei and plastids, but appeared to occur in a patchy distribution throughout the cytoplasm. With longer periods of observation, new clusters of bright pixels were seen to emerge spontaneously, and some of the clusters expanded gradually, whereas others shrank. On average, the index of cytoplasmic motility of such samples increased rapidly with time.

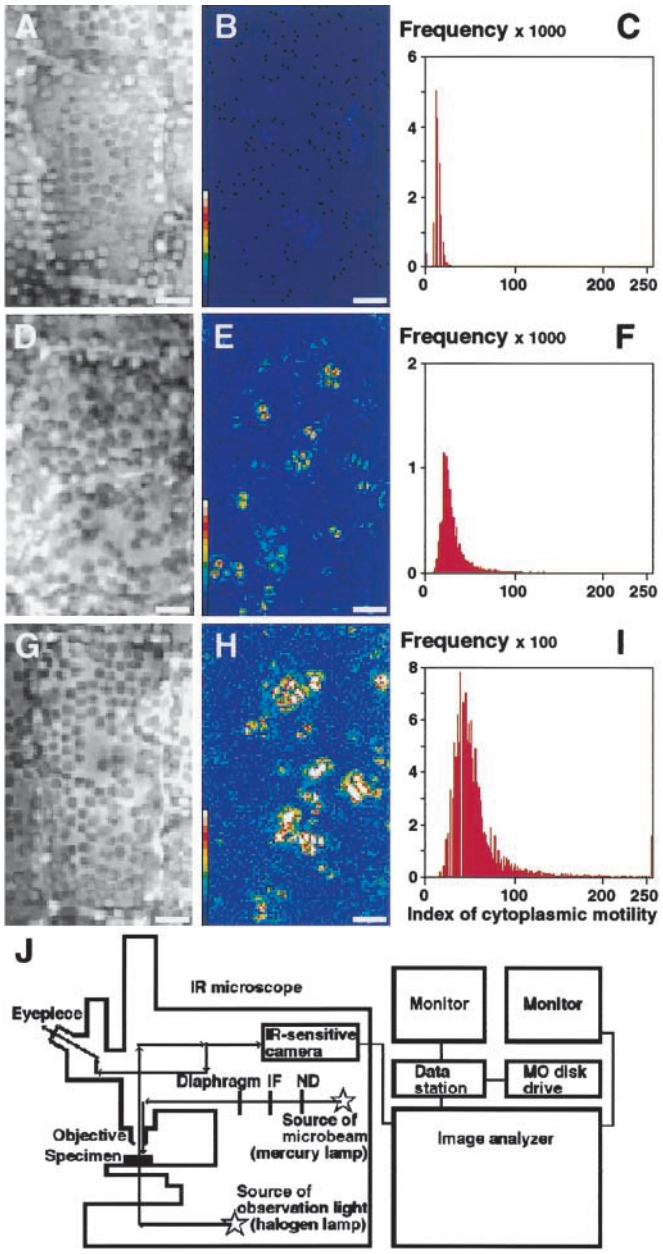

Figure 1. Quantitative Demonstration of Cytoplasmic Motility in Epidermal Cells of Vallisneria.

From samples in which different degrees of cytoplasmic motility had been induced (**[A]**, **[D]**, and **[G]**), nine serial optical images were recorded under IR light at intervals of 1.0 s. After digitization of the images, the standard deviation of brightness was determined on each pixel at the same position on the images using the dynamic image-processing procedures. Three different results are shown as processed images in false color (**[B]**, **[E]**, and **[H]**) and as frequency distributions of the calculated index (**[C]**, **[F]**, and **[I]**). The total number of pixels examined was 17,145 in each case. The abscissa and ordinate in **(C)**, **(F)**, and **(I)** show the calculated index and the number of pixels, respectively. The color scale in **(B)**, **(E)**, and **(H)** shows the values of the calculated index in 15 steps and ranges from <17 (dark blue) to 238 to 255 (white). Bars $= 5$ μm. A diagram of the microscope equipped with the microimage analyzer is shown in **(J)**. The optical image of the objective under IR light is channeled through an IR light–sensitive camera into the computer and stored sequentially on magneto-optical (MO) disks. Actinic light was applied to the sample from above through the objective. When necessary, the sample was exposed to microbeam irradiation using a diaphragm. IF, interference filter; ND, neutral density filter.

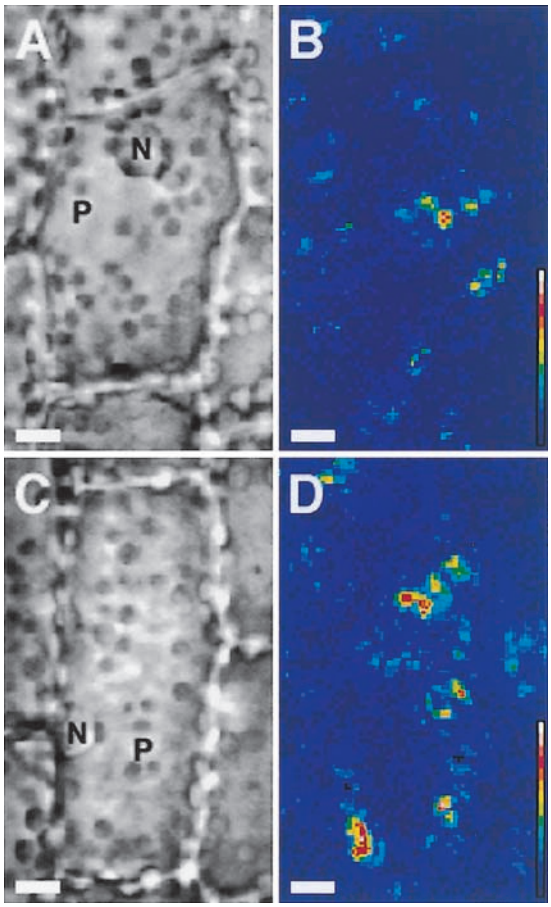

Figure 2. Quantitative Visualization of the Photoinduction of Cytoplasmic Motility in Epidermal Cells of Vallisneria.

After dark incubation for 12 to 18 h, samples were irradiated for 4 s with white light at 0.1 W/m^2 **(A)** or 2.0 W/m^2 **(C)**. Immediately after the termination of the irradiation, nine serial optical images were recorded sequentially under IR light at intervals of 1.0 s. Dynamic image processing was performed on each sample (**[B]** and **[D]**) as described in the legend to Figure 1. See the legend to Figure 1 for an explanation of the color scale. N, nucleus; P, plastid. Bars = 10 μm.

Regulation of Cytoplasmic Motility by Type II Phytochrome

Dark-adapted samples were irradiated for 1.0 s with monochromatic blue (460 nm), green (520 nm), red (660 nm), and far-red (760 nm) light of 100 μmol·m^{-2}·s^{-1}. Immediately after these light treatments, optical images of each sample were recorded under IR light (850 nm) and analyzed by the image-processing method. The resulting index of cytoplasmic motility indicated that red light was most effective at increasing the index, whereas blue light exhibited a much smaller effect and green and far-red light showed almost no effect (Table 1). The effect of red light (100 μmol·m^{-2}·s^{-1} for 1.0 s) was canceled by a subsequent irradiation with far-red light of the same fluence as the red light. The effects of red and far-red light were repeatedly reversible upon the alternation of irradiation with red and far-red light (Table 1).

After samples were irradiated with red light of 10 to 10^3 μmol·m^{-2}·s^{-1} for different time periods (0.1 to 5.0 s), we determined the magnitude of the response and plotted the resulting values against the fluence of applied light (Figure 3). The response was inducible at a fluence of 30 μmol/m^2 and reached saturation at ~1 mmol/m^2. The photoreversible effect (Table 1) and the effective range of fluences (Figure 3) strongly suggested that a type II phytochrome (Furuya, 1993) regulated the cytoplasmic motility in the epidermal cells of Vallisneria. However, there was no indication of the involvement of type I phytochrome in this effect because far-red light alone failed to induce detectable cytoplasmic motility (Table 1).

Time Requirement for the Photoinduction of Cytoplasmic Motility

Dark-adapted samples were irradiated with red or far-red light for 0.25, 0.5, or 1.0 s at a fixed fluence of 2 mmol/m^2. To determine when the effect of light on cytoplasmic motility was first detectable, we recorded optical images of the sample cells under the IR microscope sequentially at intervals of 0.2 s immediately after the termination of the pulse irradiation, as illustrated in Figure 4B. From a series of sets of nine IR light images, processed images were obtained se-

Table 1. Effects of Monochromatic Irradiation on Cytoplasmic Motility in Dark-Adapted Epidermal Cells of Vallisneria

Monochromatic Irradiation (nm)	Increase in the Index of Cytoplasmic Motility
460	0.16 ± 0.08[a]
520	0.05 ± 0.01[a]
660	0.72 ± 0.21
760	0.08 ± 0.04[a]
660, 760	0.08 ± 0.07[a]
660, 760, 660	0.72 ± 0.19

After incubation in darkness for 12 to 18 h, samples were irradiated with monochromatic light of each wavelength for 1.0 s at 100 μmol·m^{-2}·s^{-1}. The magnitude of the response was determined by subtracting the index of cytoplasmic motility determined immediately before the start of actinic irradiation from the index determined immediately after the termination of the irradiation. For each irradiation test, the response is expressed as the average of results obtained from six different samples with the standard error.

[a] Significantly different from the value obtained at 660 nm ($P < 0.05$).

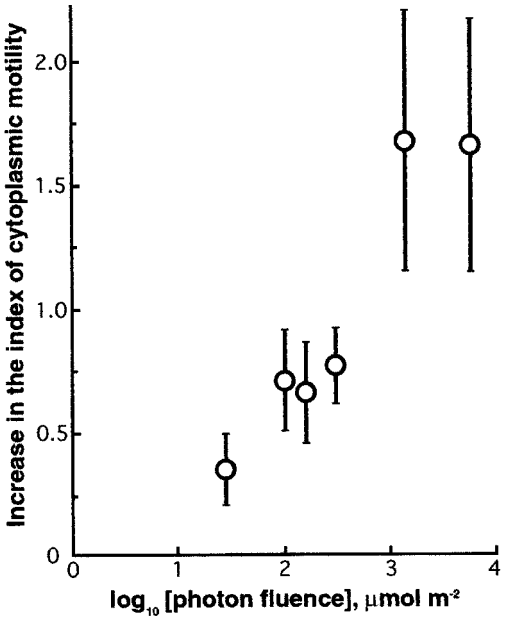

Figure 3. Fluence-Response Relationship for the Photoinduction of Cytoplasmic Motility by Red Light in Epidermal Cells of Vallisneria.

Dark-adapted samples were irradiated with light at 660 nm at various fluence rates for 0.1 to 5.0 s. The magnitude of the response was determined as described in Table 1, and it was plotted against the fluence of light at 660 nm. For each fluence rate, the response is given as the average of results obtained from two to seven different specimens with the standard error.

quentially with intervals of 0.2 s. The interval of 0.2 s was chosen because it was the shortest period of time for which it was possible to determine the index of cytoplasmic motility with an acceptable signal-to-noise ratio.

In the case of red light irradiation for 0.25 s, the first processed image (Figure 4A, R0.25, top) was obtained after calculation of the index of cytoplasmic motility using the first set of nine serial IR light images that were recorded at 0.25, 0.45, 0.65, 0.85, 1.05, 1.25, 1.45, 1.65, and 1.85 s after the start of red light irradiation (Figure 4B). The next image (Figure 4A, R0.25, second from top) was obtained using the next set of nine serial IR light images recorded at 0.45 to 2.05 s. Such image-processing procedures were performed successively at intervals of 0.2 s with the sets of nine serial IR light images (Figure 4A, R0.25). No prominent change in the index of cytoplasmic motility was detected in the top four processed images (shown in false color), indicating that the magnitude of cytoplasmic motility did not change substantially from the dark-adapted level in the first 2.45 s after the start of the red light irradiation. By contrast, a cluster of bright pixels became evident in the fifth processed image and thereafter (Figure 4A, R0.25), indicating that the first significant changes in pixel brightness occurred in the last IR light image, captured 2.65 s after the start of pulse irradiation with red light.

In the case of red light irradiation for 0.5 s (Figure 4A, R0.5), a cluster of bright pixels first became evident in the fourth processed image, whereas in the case of a 1.0-s red light pulse (Figure 4A, R1.0), cytoplasmic movement was first seen in the second processed image. These results represent the induction of significant cytoplasmic movement at 2.7 and 2.8 s after the start of the 0.5- and 1.0-s red light pulse, respectively. In repeated experiments, we found that the earliest change in the cytoplasmic motility detectable in processed images occurred at ~2.0 to 2.5 s after the start of actinic irradiation with red light (Table 2). Thus, the Bunsen-Roscoe reciprocal law held in this rapid response, and the photoregulation of cytoplasmic motility was shown to be the earliest response to a light stimulus among known responses under the control of type II phytochrome.

When far-red light was applied for 0.5 s immediately after irradiation with red light for 0.25 s, the induction of cytoplasmic motility was not observed (Figure 4A, R0.25/FR0.5). Irradiation with far-red pulse light and the observing IR light did not produce any changes in the processed images for the period of these experiments (Figure 4A, FR0.5 and IR). This finding confirmed our previous conclusion that the photoregulation of cytoplasmic motility is controlled by type II phytochrome but not by type I phytochrome.

Effects of Microbeam Light on Cytoplasmic Motility

Using a microbeam irradiation technique, we next examined whether the phytochrome-induced signal regulating cytoplasmic motility could be transmitted from cell to cell. When a selected cell was irradiated for 5 s with a localized spot of red light (100 $\mu mol \cdot m^{-2} \cdot s^{-1}$, 15 μm in diameter) (Figure 5A), the index of cytoplasmic motility in the irradiated cell increased rapidly (Figure 5B), whereas its neighboring unirradiated cells did not respond during this experiment (Figures 5C and 5D), suggesting that any light-induced signal was not spread from the irradiated cell to the surrounding area. The cluster of bright pixels induced in the irradiated area disappeared completely within several minutes.

Indices of cytoplasmic motility were determined for both microbeam-irradiated and unirradiated cells. Although microbeam irradiation did not always produce a significant increase in the index in the irradiated cell, the results clearly showed that when the response was detected, it was limited exclusively to irradiated cells and there was no indication of any long-distance signaling through the leaf tissue (Table 3, experiments 1 and 2). Moreover, even in a single cell, the red light–induced signal did not spread from the irradiated region to neighboring regions (Table 3, experiment 3). The effect of a microbeam of red light was antagonized almost completely by subsequent irradiation with far-red light (data not shown). In these experiments, changes in the cytoplasmic motility index were exaggerated compared with those in

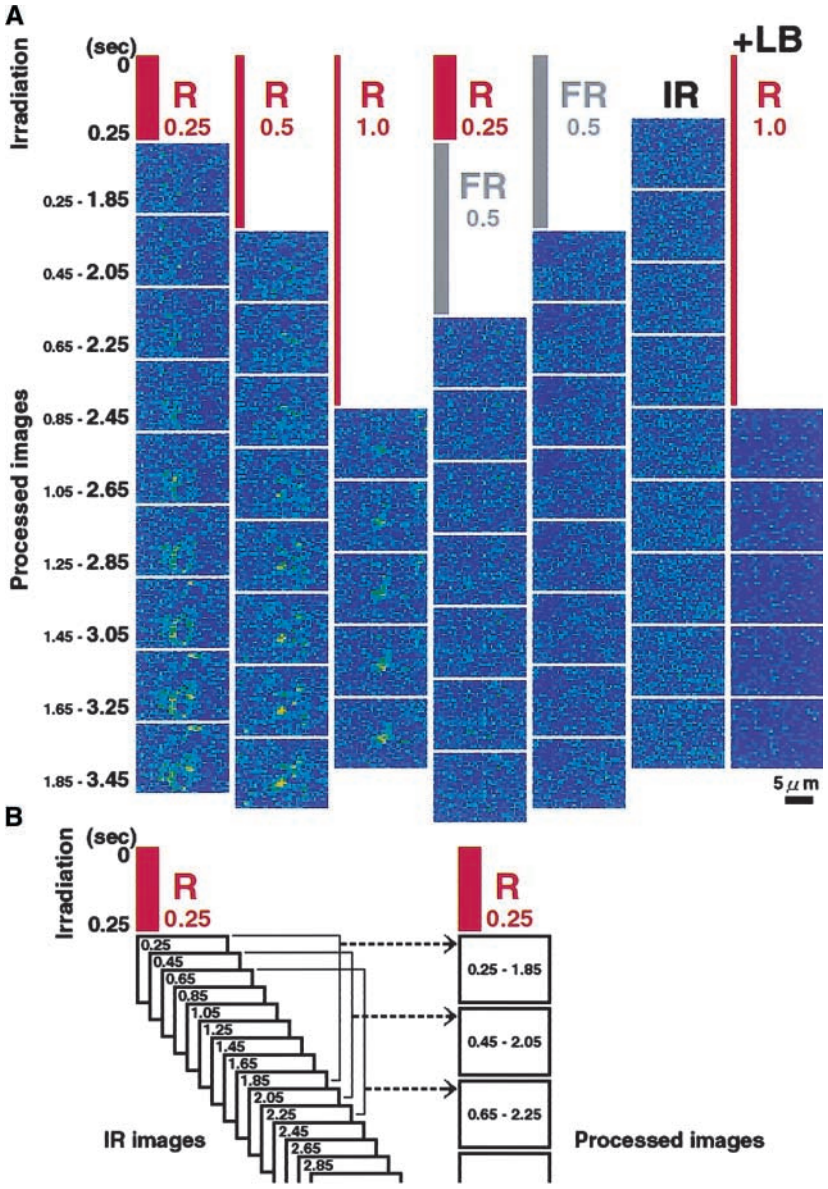

Figure 4. Time Course of the Photoinduction of Cytoplasmic Motility in Epidermal Cells of Vallisneria.

Dark-adapted samples were irradiated with red (R) or far-red (FR) light for different periods of time at a fixed fluence of 2 mmol/m^2 (irradiation in **[A]**). Immediately after the termination of each pulse irradiation, optical images were recorded sequentially under IR light at intervals of 0.2 s, as illustrated schematically in **(B)**. From a series of nine such serial images, the individual processed images were obtained sequentially at intervals of 0.2 s (processed images in **[B]**). +LB, irradiation in the presence of 0.1 μM latrunculin B. Bar = 5 μm.

the whole irradiation experiments (Table 1). This finding is attributable to the fact that measurements were made only in the samples that responded to microbeam irradiation and were based on a much smaller number of pixels. In the whole irradiation experiments, the index was determined for a large area that included several cells, of which the whole outer periclinal layer had been irradiated. Because the light-induced cytoplasmic motility occurred in a patchy manner (Figure 2), the average indices became much smaller compared with those in the microbeam irradiation experiments.

Immunochemical Detection of Phytochromes in Vallisneria

To demonstrate that the material used in the present study does contain phytochrome(s), we first prepared extracts of soluble proteins from dark-adapted whole leaves of Vallisneria and performed immunoprecipitation with eight monoclonal anti-phytochrome antibodies produced previously against different phytochromes from various plants (Table 4). Immunoblot analysis revealed that polypeptides of ~120 kD (as determined by SDS-PAGE) were precipitated with those specific antibodies, and the precipitated polypeptides exhibited different immunoaffinity to the individual antibodies (Figure 6A). Furthermore, Zn^{2+}-induced luminescence signal was evident in all 120-kD bands precipitated with the anti-phytochrome antibodies (Figure 6B), suggesting that the anti-phytochrome antibody–responsive polypeptides incorporated a bilin chromophore. Using the anti-PHYB antibodies mBA02 and mBP01, we further confirmed that the antibody-responsive polypeptides of 120 kD also were precipitated from the protein extract prepared from dark-adapted epidermal tissues (Figure 6C). The molecular mass of these polypeptides was consistent with that of the previously reported type I and type II phytochromes in other plant species, which ranged from 118 to 125 kD (Furuya, 1993), lending further support to the conclusion that Vallisneria leaf epidermal cells contain phytochrome(s).

Because the anti-PHYB antibodies seemed to have higher affinity for Vallisneria phytochrome(s) than the anti-PHYA antibodies (Figure 6), we used those antibodies as the primary antibody to perform immunocytochemical assays on cryosections prepared from the dark-adapted Vallisneria leaves. Strong immunosignals were observed in the symplastic region of the epidermal cells with monoclonal antibodies mBA01 (Figure 7A), mBA02 (Figure 7B), and mBP01 (Figure 7C), all of which positively detected the 120-kD polypeptide in immunoprecipitation (Figure 6). By contrast, only very weak immunosignals were detectable with mBT04 (Figure 7D). With nonimmune serum, no signal was detected (Figure 7E).

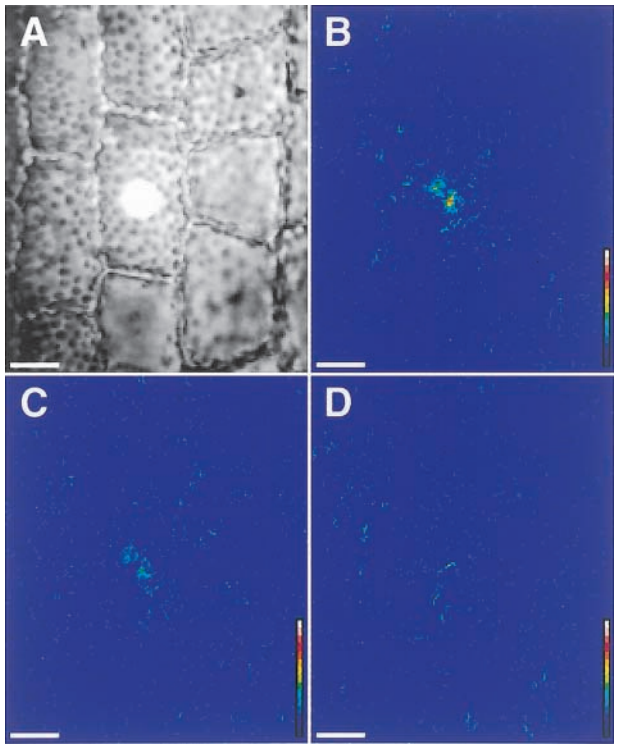

Figure 5. Induction of Cytoplasmic Motility by Microbeam Irradiation in Epidermal Cells of Vallisneria.

One epidermal cell was irradiated with red light of 100 μmol·m^{-2}·s^{-1} for 5.0 s via a microbeam of 15 μm in diameter **(A)**. The calculated images were obtained from 0 to 8 s **(B)**, 120 to 128 s **(C)**, and 240 to 248 s **(D)** after the termination of actinic irradiation. To demonstrate the response clearly, calculated standard deviations were multiplied by a constant larger than the ordinary one (32). See the legend to Figure 1 for an explanation of the color scale. Bars = 20 μm.

Table 2. Time Required for the Photoinduction of Cytoplasmic Motility in Epidermal Cells of Vallisneria

Experiment 1		Experiment 2	
Order of Image Processing (s)	Number of Samples Responding	Order of Image Processing (s)	Number of Samples Responding
1 (0.25 to 1.85)	0		
2 (0.45 to 2.05)	0	1 (0.5 to 2.1)	0
3 (0.65 to 2.25)	4	2 (0.7 to 2.3)	1
4 (0.85 to 2.45)	1	3 (0.9 to 2.5)	2
5 (1.05 to 2.65)	0	4 (1.1 to 2.7)	1
6 (1.25 to 2.85)	1	5 (1.3 to 2.9)	3
7 (1.45 to 3.05)	0	6 (1.5 to 3.1)	1
Later	6	Later	5

Dark-adapted samples were irradiated with red light either for 0.25 s at 6500 μmol·m^{-2}·s^{-1} (experiment 1) or for 0.5 s at 2600 μmol·m^{-2}·s^{-1} (experiment 2). Immediately after the termination of the irradiation, optical images were recorded sequentially under IR at intervals of 0.2 s. From sets of nine serial images, the individual processed images were obtained sequentially at intervals of 0.2 s. After such processed images were arranged sequentially as in Figure 4, the image with the first detectable change in the index of cytoplasmic motility was determined.

Involvement of the Actin Cytoskeleton and Calcium in Cytoplasmic Motility

Finally, we attempted to characterize a motile apparatus that drives cytoplasmic motility in Vallisneria. Processed images

Table 3. Effects of Microbeam Irradiation on Cytoplasmic Motility in Epidermal Cells of Vallisneria

Effect	Experiment 1	Experiment 2	Experiment 3
Irradiated cell or region	20.5 ± 11.3[a]	30.2 ± 23.8[a]	25.0 ± 10.1[a]
Adjacent cells or regions			
Distal	13.5 ± 4.9	13.6 ± 4.0	16.1 ± 5.6
Proximal	14.5 ± 5.4	14.2 ± 3.5	12.6 ± 4.5
Right side	13.8 ± 6.3	13.3 ± 4.0	11.3 ± 4.7
Left side	12.9 ± 6.5	14.0 ± 3.6	12.0 ± 4.4
Distant cell or region	14.2 ± 5.1	13.5 ± 3.4	14.8 ± 4.2
Diameter of microbeam	50 μm	10 μm	5 μm
Duration of irradiation	5 s	1 s	1 s
Number of pixels examined	3363	225	49

A part of one epidermal cell in a dark-adapted sample was irradiated with red light of 100 $\mu mol \cdot m^{-2} \cdot s^{-1}$ using the microirradiation system. The index of cytoplasmic motility was determined immediately after the termination of actinic irradiation on the irradiated cell or region and several neighboring cells or regions in the same optical field. For each experiment, the responses are expressed as the average of the index of cytoplasmic motility obtained from pixels in a defined area with the standard deviation. In experiment 3, the magnitude of response was compared between the irradiated region and the adjoining unirradiated regions in the same cell.

[a] Significantly different from other cells or regions ($P < 0.001$).

were obtained sequentially from dark-adapted samples under IR light, in which numerous tiny clusters of pixels with very small indices of cytoplasmic motility emerged and disappeared spontaneously. On average, the index of such samples remained at a constant level. When such samples were treated with latrunculin B or cytochalasin B in darkness, the index declined dramatically (Table 5, experiment 1). In the processed images of those treated samples, we observed no spontaneous appearance and disappearance of tiny clusters of pixels with very small indices of cytoplasmic motility. Moreover, in the presence of latrunculin B or cytochalasin B, light irradiation did not induce any increase in the index of cytoplasmic motility (Table 5, experiment 1). By staining with fluorescently labeled phalloidin, we confirmed that the actin filaments along the outer periclinal walls of epidermal cells were destroyed almost completely after treatment with latrunculin B (Figure 8). In such samples, a pulse irradiation with red light did not induce a rapid increase in cytoplasmic motility (Figure 4A, +LB).

When latrunculin B and cytochalasin B were removed by washing, the effects disappeared and the index returned to the level of the dark-adapted samples (Table 5, experiment 1). Furthermore, in the washed samples, the responsiveness to light irradiation was recovered fully. Another inhibitor, cytochalasin D, exhibited quite similar effects at 0.1 mM (data not shown). By contrast, the microtubule-disrupting reagent colchicine affected neither the dark-adapted index of cytoplasmic motility nor the responsiveness to light irradiation (Table 5, experiment 1). These results strongly suggest that the observed cytoplasmic motility is an active process driven by an actin-dependent motile apparatus and that the movement of the cytoplasm with very small amplitude can occur in a patchy manner even in complete darkness.

When the dark-adapted samples were treated with the Ca^{2+}-chelating reagent 1,2-bis(*o*-aminophenoxy)ethane-*N*,*N*,*N*,*N*-tetraacetic acid or EGTA, the induction of cytoplasmic motility was observed even in darkness (Figure 9). The effects of Ca^{2+}-chelating reagents were canceled when those reagents were applied with a high concentration of Ca^{2+}. Although these results suggested the possible involvement of Ca^{2+} in the regulation of cytoplasmic motility in the material studied here, the photoinduction of cytoplasmic motility did not seem to be affected by an inhibitor of plasma membrane ATPase (vanadate) or by a plasma membrane Ca^{2+} channel blocker (La^{3+}) (Table 5, experiment 2).

DISCUSSION

Model for the Rapid Regulation of Cytoplasmic Motility by Phytochrome

In this study, we have established a new method to quantify and visualize cytoplasmic motility using an IR microscope combined with a dynamic image-processing procedure. Furthermore, the microirradiation equipment enabled a precise spatiotemporal analysis of the photoregulation of the cytoplasmic motility. From the results obtained, we propose

Table 4. Monoclonal Antibodies Used in the Immunochemical Analyses

Antibodies	Specificity	Reference
mBA01, mBA02	Specific to Arabidopsis phytochrome B	Shinomura et al., 1996
mBP01	Specific to pea phytochrome B	López-Juez et al., 1992
mBT04	Specific to tobacco phytochrome B and pea phytochrome B	López-Juez et al., 1992
mAA01, mAA02	Specific to Arabidopsis phytochrome A	Shinomura et al., 1996
mAR07, mAR14	Specific to rye phytochrome A and rice phytochrome A	Nagatani et al., 1991

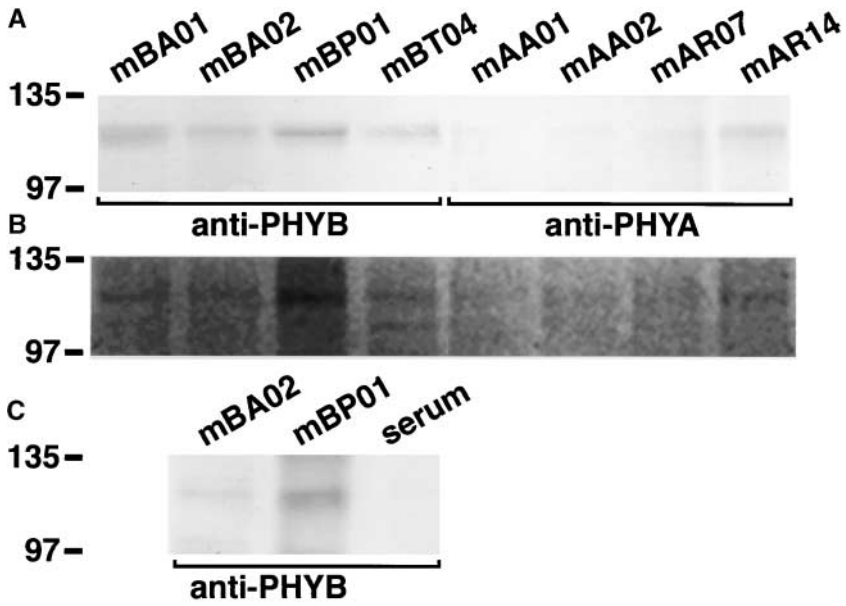

Figure 6. Immunoblot and Zinc Blot Analysis of the Immunoprecipitated Vallisneria Phytochrome(s).

Anti-phytochrome antibody–responsive polypeptides were immunoprecipitated from the protein extract prepared from dark-adapted whole leaves **(A)** or epidermal tissues **(C)**. The precipitated polypeptides were separated by SDS-PAGE and detected with monoclonal antibodies specific to PHYB, a mixture of mBA01 and mBT04 (anti-PHYB in **[A]** and **[C]**), or to PHYA, a mixture of mAA01 and mAR14 (anti-PHYA in **[A]**). Zn^{2+}-induced luminescence from bilin chromophore was visualized on the duplicated gels using an image analyzer **(B)**. Molecular mass is indicated at left in kD. Serum indicates control using nonimmune serum.

the following hypothesis for the phytochrome regulation of cytoplasmic motility in Vallisneria epidermal cells. Phototransformation of the red light–absorbing form of type II phytochrome, which is located in the cytoplasm, to the far-red light–absorbing form produces an altered interaction with a cytoplasmic partner, such as the PKS1 protein characterized previously in Arabidopsis (Fankhauser et al., 1999). This change evokes a modulation in the cytoplasmic level of Ca^{2+}. Ca^{2+} interacts with Ca^{2+}-sensitive cytoskeletal factors, which might include the motor protein myosin (Yokota et al., 1999), which is known to function in the generation of motive force through an interaction with actin filaments and the Ca^{2+}-sensitive actin binding protein (Yokota et al., 2000) necessary for the reorganization of actin filaments. Transduction of the type II phytochrome-dependent signals onto the actin-based motile apparatus is completed within 2.5 s after the start of light irradiation only in the light-exposed cytoplasmic region.

Cytoplasmic Motility under the Control of Type II Phytochrome

The red/far-red light reversibility (Table 1) and the light requirement revealed by the fluence-response curve (Figure 3) for the photoinduction of cytoplasmic motility are consistent with the known properties of a type II phytochrome. Because similar effects of red and far-red light on cytoplasmic motility were observed in the presence of DCMU, the inhibitor of photosynthetic electron transport (data not shown), photosynthesis does not seem to be involved in the response. With respect to the possible effects of type I phytochrome, we detected no rapid effects of far-red light on cytoplasmic motility (Table 1, Figure 4A). Nevertheless, considering the fact that a brief irradiation with 10 nmol/m^2 red light photoirreversibly induces the phytochrome A–dependent germination of Arabidopsis seeds (Shinomura et al., 1996), the possible involvement of a very-low-fluence response under the control of type I phytochrome cannot be excluded.

Rapidly Photoinducible Responses in Plant Cells

Several rapid responses in plant cells to red light (Racusen, 1976; Newman, 1981; Ermolayeva et al., 1996) and blue light (Nishizaki, 1988; Lewis et al., 1997) have been identified using electrophysiological procedures. Among these studies, an involvement of phytochrome as the photoreceptor

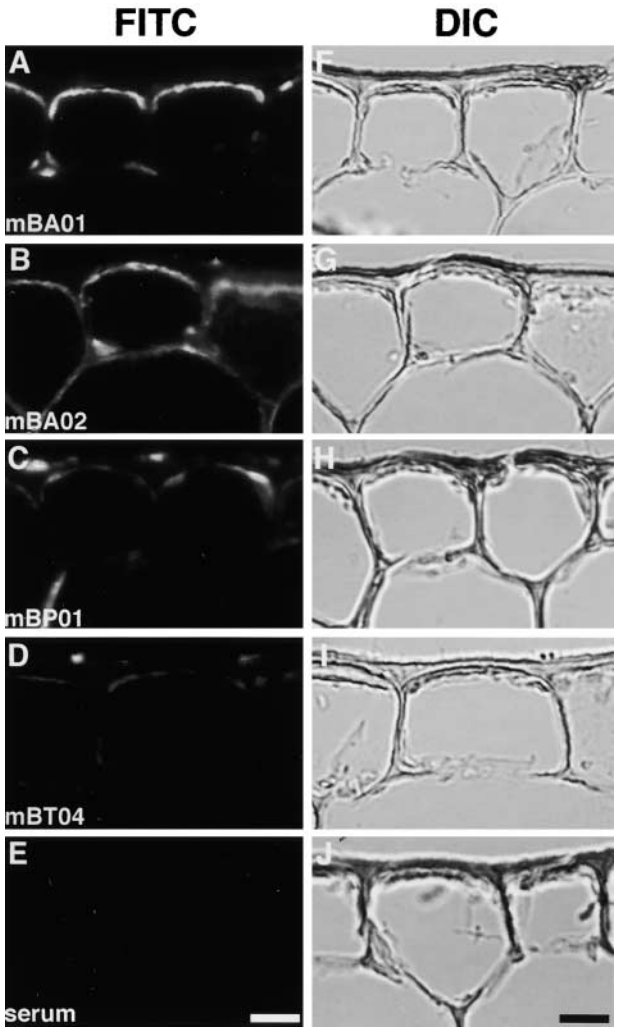

Figure 7. Immunocytochemical Analysis of Anti-Phytochrome Antibody–Responsive Polypeptides in Epidermal Cells of Vallisneria.

Cryosections were prepared from the dark-adapted leaf epidermis. The immunosignals from anti-phytochrome antibody–responsive polypeptides were visualized by indirect immunofluorescence microscopy using monoclonal anti-PHYB antibodies. On each section, the epi-fluorescence image (FITC; **[A]** to **[E]**) and the differential interference contrast image (DIC; **[F]** to **[J]**) were demonstrated. Serum indicates control using nonimmune serum. Bars = 20 μm.

was demonstrated unequivocally only in the cases of *Avena* coleoptiles (Quail, 1983) and *Physcomitrella* caulonemal cells (Ermolayeva et al., 1996). In *Avena* coleoptiles, Newman (1981) analyzed the initial processes of red light–induced changes in the surface potential and found a lag time of 4.5 s between the start of actinic irradiation and the first electrical change. In *Physcomitrella* caulonemata, the first change in red light–induced depolarization was detectable within 2 to 15 s (Ermolayeva et al., 1996). Although we did not examine whether the photoinduction of cytoplasmic motility involves any changes in membrane properties, some interaction of the phytochrome-dependent signals with the plasma membrane is suggested because the response was localized only to the cytoplasmic region exposed to red light even in the irradiated single cell (Figure 5, Table 3). In any case, the photoinduction of cytoplasmic motility in epidermal cells of Vallisneria can be categorized as one of the most rapid responses under the control of type II phytochrome reported to date.

Localized Responses and Long-Distance Signaling in Phytochrome-Mediated Regulation

Our demonstration of the localized regulation of cytoplasmic motility (Figure 5, Table 3) indicates that microbeam-irradiated single cells are fully equipped with all of the components required for the response: the photoreceptor phytochrome, components for signal transduction, and the effector actin cytoskeleton. In phytochrome-dependent intracellular movements, localized induction of a new type of movement has been reported. Haupt et al. (1969) showed that in the green algae *Mougeotia*, microbeam irradiation of a tiny part of the cortical cytoplasm induced a rotation of the ribbon-shaped chloroplast only in the vicinity of the irradiated part. Orientational migration of chloroplasts to the microbeam-irradiated area in a single cell was demonstrated in prothallial cells of the fern *Adiantum* (Kagawa and Wada, 1994). These observations all suggested that, to induce such localized movements, the photoreceptor molecules might be anchored in the vicinity of the plasma membrane (Haupt et al., 1969; Wada et al., 1993). In animal cells, the involvement of the cytoskeleton in the maintenance of domain structures composed of receptor molecules on the plasma membrane has been investigated (Kusumi and Sako, 1996). Such mechanisms should be investigated with regard to the localization of the plant photoreceptor molecules.

By contrast, phytochrome in the cotyledons of *Sinapis* (Nick et al., 1993) and tobacco (Bischoff et al., 1997; Schütz and Furuya, 2001) transmits an intercellular, long-distance signal from the microbeam-irradiated cell(s) to other cells throughout the treated cotyledon. It remains to be determined whether these long-distance signal-dependent responses occur downstream of the induction of cytoplasmic motility or in different branches of a cascade.

Actin-Dependent Cytoplasmic Motility and Its Regulation by Ca^{2+}

Intracellular movements in plant cells are driven by a well-organized motile apparatus (Nagai, 1993; Wada et al., 1993), which is composed predominantly of actin microfila-

Table 5. Effects of Various Inhibitors on Cytoplasmic Motility in Epidermal Cells of Vallisneria

Experiment 1	*n*	After Treatment	+WL	After Wash	+WL
Control	5	14.1 ± 0.4	16.2 ± 0.5		
Latrunculin B	5	11.9 ± 0.3[a]	11.8 ± 0.4	14.0 ± 0.5	17.2 ± 0.5
Cytochalasin B	4	12.1 ± 0.1[a]	12.0 ± 0.3	14.0 ± 0.6	16.9 ± 1.3
Colchicine	5	14.2 ± 0.4	16.5 ± 0.7		
Experiment 2	*n*	After Treatment	+R		
Control	3	13.9 ± 0.9	15.2 ± 1.0		
Vanadate	5	13.8 ± 1.2	15.1 ± 1.2		
La^{3+}	5	13.8 ± 0.9	15.3 ± 1.1		

Dark-adapted samples were treated in darkness with 0.1 μM latrunculin B for 1 h, 0.1 mM cytochalasin B for 3 h, 1 mM colchicine for 6 h, 0.2 mM vanadate for 1 h, or 0.1 mM La^{3+} for 1 h. In the treated samples, the index of cytoplasmic motility was determined immediately before and after irradiation with white light (+WL; 2 W/m^2, 4 s) or red light (+R; 100 μmol·m^{-2}·s^{-1}, 1 s). After treatment with latrunculin B and cytochalasin B, the reagent was removed by vigorous washing of the treated samples with artificial pond water for 2 or 4 h, respectively, and then the photoinduction of cytoplasmic motility was examined in the washed samples. For each treatment, the response is expressed as the average with the standard error. Control, treatment with normal artificial pond water; *n*, the number of samples examined.

[a] Significantly different from the initial value of the index (13.9 ± 0.2) determined immediately before the start of treatment with reagents ($P < 0.02$).

ments (Staiger, 2000) and microtubules (Nick, 1998), as in animal cells. Although cytoplasmic motility has been described occasionally in the literature and can be modulated by light (Schönbohm, 1972; Takagi and Nagai, 1985; Kagawa and Wada, 2000), no study has investigated the nature of the mechanism driving this motility. In this study, we have obtained quantitative data to show that the cytoplasmic motility in epidermal cells of Vallisneria can be inhibited reversibly by latrunculin B and cytochalasins (Table 5, experiment 1). Actin filaments in epidermal cells of Vallisneria run as a parallel array of thin bundles in the vicinity of the plasma membrane (Yamaguchi and Nagai, 1981). These bundles form the configuration of a network over the cytoplasmic layer along the outer periclinal walls (Dong et al., 1998) (Figure 8A). Furthermore, we had shown previously that cytochalasin B has a specific, destructive effect on actin filaments and exhibits no apparent side effect in these cells (e.g., on the viscosity of cytoplasm) (Dong et al., 1998). Consequently, it is evident that the cytoplasmic motility in the material examined here is driven by the actin-based motile apparatus.

Because the exogenous application of Ca^{2+}-chelating reagents has been demonstrated to effectively modulate cytoplasmic Ca^{2+} in plant cells using a fluorescent probe (Gilroy et al., 1991) and a calcium precipitant (Takagi and Nagai, 1983), the induction of cytoplasmic motility by treatment of the dark-adapted samples with Ca^{2+}-chelating reagents (Figure 9) strongly suggests a Ca^{2+}-dependent regulation of cytoplasmic motility. A rapid regulation by Ca^{2+} of actin-based cytoplasmic streaming has been investigated extensively in characean cells (Tazawa and Shimmen, 1987). Although a motor protein myosin was postulated as one of the targets for Ca^{2+}, biochemically isolated myosin from the characean cells has not exhibited Ca^{2+} sensitivity to date (Awata et al., 2001). On the other hand, the involvement of

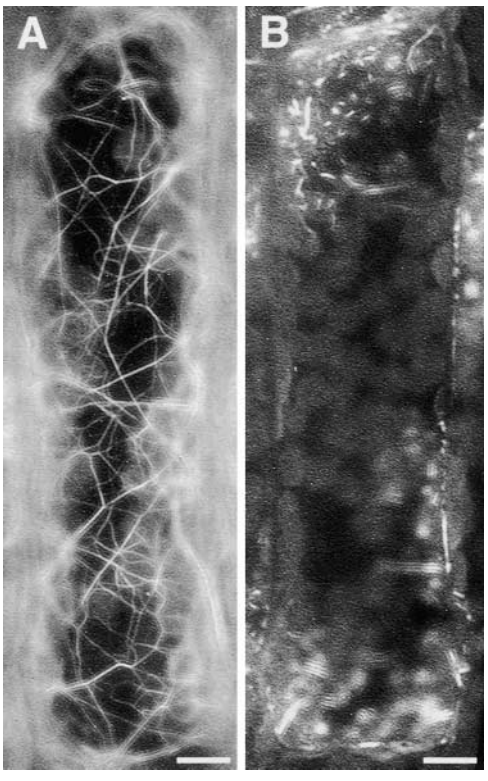

Figure 8. Effects of Latrunculin B on the Configuration of Actin Filaments in Epidermal Cells of Vallisneria.

Actin filaments on the outer periclinal walls of dark-adapted epidermal cells were visualized by staining with fluorescently labeled phalloidin before **(A)** and after **(B)** treatment with 0.1 μM latrunculin B for 1 h. Bars = 10 μm.

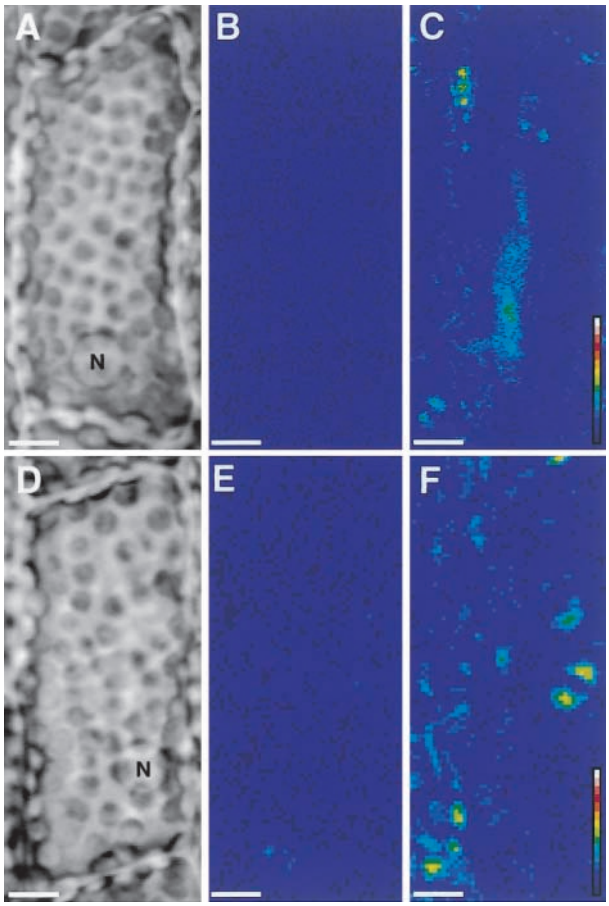

Figure 9. Induction of Cytoplasmic Motility by Ca^{2+}-Chelating Reagents in Epidermal Cells of Vallisneria.

Dark-adapted samples (**[A]** and **[D]**) were treated with either 1 mM 1,2-bis(*o*-aminophenoxy)ethane-*N*,*N*,*N*,*N*-tetraacetic acid (BAPTA) or 0.1 mM EGTA in darkness. Optical images were recorded under IR light before (**[B]** and **[E]**) and after either 15 min of treatment with BAPTA **(C)** or 5 min of treatment with EGTA **(F)**. Dynamic image processing was performed as described in the legend to Figure 1. See the legend to Figure 1 for an explanation of the color scale. N, nucleus. Bars = 10 μm.

Ca^{2+} influx across the plasma membrane in the rapid inhibition of cytoplasmic streaming upon mechanical or electrical stimulation has been established (Williamson and Ashley, 1982; Kikuyama and Tazawa, 1983). In the present study, however, potent inhibitors for the influx and efflux of Ca^{2+} across the plasma membrane did not exhibit any significant effects on the photoinduction of cytoplasmic motility in the epidermal cells of Vallisneria (Table 5, experiment 2), suggesting an involvement of intracellular Ca^{2+} stores. In conclusion, we propose that a Ca^{2+}-sensitive actin cytoskeleton provides a cytoplasmic scaffold for certain early steps in the pathway of phytochrome-dependent signal transduction in plant cells.

METHODS

Plant Material and Preparation of Specimens

Young plants of *Vallisneria gigantea* were cultured in buckets filled with tap water, with soil on the bottom, under a daily regime of 12 h of light (0.5 W/m^2) and 12 h of darkness at 20 to 25°C. The light source was a bank of 20-W fluorescent lamps (FL20S-PG; National, Kadoma, Japan). The procedures for the preparation of specimens were described in detail previously (Dong et al., 1995). In brief, adaxial pieces of leaf 5 to 10 mm in width and 2 to 3 mm in length were removed at the end of a light period. Each piece was floated in artificial pond water, which contained 0.5 mM KCl, 0.2 mM NaCl, 0.1 mM $Ca(NO_3)_2$, 0.1 mM $Mg(NO_3)_2$, and 2 mM Pipes, pH 7.0, for one cycle of darkness and light, and then it was mounted on a glass slide. The glass slide was immersed in fresh artificial pond water in a Petri dish and kept in complete darkness for another 12 to 18 h. Stock solutions of latrunculin B and cytochalasin B were prepared in DMSO and diluted with artificial pond water before use.

Light Treatments

After incubation in complete darkness for 12 to 18 h, a sample was placed on the stage of a custom-constructed IR microscope (FR-1; Olympus, Tokyo, Japan), as shown in Figure 1J. Epidermal cells were irradiated with actinic light, from above, through the light path of the epi-illumination system. Monochromatic blue (460 nm), green (520 nm), red (660 nm), and far-red (760 nm) light was produced by appropriate combinations of an interference filter and a cutoff filter. The filters were placed in the light path in front of a mercury lamp (USH-102D; Ushio, Inc., Tokyo, Japan). The duration of actinic irradiation was controlled by an electric shutter (YLI SC-1; Olympus). When a single cell was irradiated, a diaphragm with holes of different diameters was placed in the light path of the epi-illumination system. Light through each hole could be focused correctly on the focal plane of the objective of the light microscope as a microbeam. The fluence rate of monochromatic light was controlled with neutral density filters, and it was measured with a silicon photodiode (S1337-1010BQ; Hamamatsu Photonics, Hamamatsu, Japan).

Dynamic Processing of Digital Images

A layer of cytoplasm along the outer periclinal walls of an epidermal cell was brought into focus under IR light with a ×40 objective with a numerical aperture of 0.70. Several epidermal cells could be observed simultaneously in the same optical field. Optical images of the specimen were fed sequentially into a computer (ATX-7001; Epson Direct, Tokyo, Japan) at appropriate intervals through an IR light–sensitive camera (C2400-08; Hamamatsu Photonics) and stored on magneto-optical disks. The stored images were processed using an improved version of earlier custom-made software (Mineyuki et al., 1983).

The brightness of each pixel on each optical image was assigned one of 256 levels. From an appropriate number of such images, the standard deviation for all levels of brightness was calculated for individual pixels at the same position. If a pixel exhibited frequent changes in brightness, the resulting value became larger, whereas when a pixel exhibited only occasional changes in brightness, a smaller value was obtained. The calculated standard deviations were

taken as an index of cytoplasmic motility after multiplication by an appropriate constant. For the visual demonstration of cytoplasmic motility, the index of cytoplasmic motility for individual pixels was displayed as a processed image in 15-step false color. Unless noted otherwise, optical images were recorded at intervals of 1.0 s, and the index of cytoplasmic motility for individual pixels was calculated from nine serial images at the multiplying constant of 32. Thus, one processed image represented the cytoplasmic motility detected during 8.0 s of observation. When the time course of the photoinduction of cytoplasmic motility was examined (Figure 4, Table 2), optical images were recorded at intervals of 0.2 s (Figure 4B). The dimensions of each pixel were $0.8 \times 0.8\ \mu m^2$ under the experimental conditions of the present study. Except for the microbeam irradiation study (Figure 5, Table 3), the index of cytoplasmic motility was determined on 200,000 to 250,000 pixels, which covered several epidermal cells for each sample. Autofluorescence from chlorophylls was eliminated efficiently by sheets of blue cellophane (transmissible from 350 to 530 nm and >700 nm; Hino-Asahido Corp., Tokyo, Japan) placed in the light path in front of the IR light–sensitive camera. All of the experiments were performed under dim green light at 18 to 22°C.

Protein Extraction

Protein extract was prepared from either whole leaves or epidermal tissues of the leaves. In the former case, the leaves were frozen rapidly in liquid nitrogen after whole plants of Vallisneria were kept in complete darkness for 12 to 18 h. In the latter case, at the end of a light period of the daily regime, the leaves first were cut into pieces of 5 to 10 mm in width and 2 to 3 mm in length. The mesophyll tissue in each piece was removed carefully using razor blades. After such leaf pieces of epidermal tissue were floated in fresh artificial pond water for one cycle of darkness and light, they were kept in complete darkness for another 12 to 18 h and then frozen in liquid nitrogen. The frozen materials (5 g fresh weight) were pulverized at liquid nitrogen temperature with a mortar and pestle. The resulting leaf powder was homogenized further with a Polytron homogenizer (PT1200; Kinematica AG, Luzern, Switzerland) in an ice bath for 3 min with a homogenizing medium, at a ratio of 2 mL/g fresh weight, that contained 25% ethylene glycol, 70 mM $(NH_4)_2SO_4$, 7 mM Na_4EDTA, 20 mM $Na_2S_2O_5$, and 100 mM Tris-HCl, pH 8.3. A protease inhibitor cocktail (Roche Molecular Biochemicals, Mannheim, Germany) was added immediately before use. The homogenate was clarified by centrifugation at 8000*g* for 10 min at 4°C. The supernatant was brought to 0.1% (w/v) polyethyleneimine by the addition of a 10% (w/v) stock solution adjusted to pH 8.0, stirred for 5 min, and then clarified by centrifugation at 50,000*g* for 30 min at 4°C. The resulting supernatant was cleaned further by incubation with 50 μL/mL protein G–Sepharose of 50% slurry (Amersham Pharmacia Biotech, Uppsala, Sweden) for 1 h at 4°C with gentle mixing and used as the protein extract for subsequent experiments.

Immunoblot and Zinc Blot Analysis

The cleaned protein extract (of 1 mL, of which the protein content was ~1 mg/mL) was incubated with 50 μL of hybridoma tissue culture supernatant for each anti-phytochrome monoclonal antibody (Table 4) in an ice bath for 4 h with gentle mixing. After removing nonspecifically formed protein aggregates by centrifugation at 10,000*g* for 10 min at 4°C, 50 μL of protein G–Sepharose (50% slurry) was added and incubated further for 1 h. The immune complexes were collected by centrifugation at 12,000*g* for 20 s and washed three times with 1 mL of a solution that contained 150 mM NaCl, 5 mM EDTA, 0.1% Triton X-100, 0.02% SDS, and 50 mM Tris-HCl, pH 7.5, and then once more with the solution lacking Triton X-100 and SDS. After the immunoprecipitated polypeptides were suspended in 20 μL of SDS-PAGE sample buffer, 15 μL of the resulting supernatant for each sample was separated by SDS-PAGE. Anti-phytochrome antibody–responsive polypeptides were detected using monoclonal antibodies mAA01 plus mAR14 or mBA01 plus mBP01, as described previously (Shinomura et al., 1996). The duplicated gels were incubated in a solution containing 20 mM zinc acetate and 150 mM Tris-HCl, pH 7.0, for 20 min with gentle shaking and then washed twice with distilled water for 5 min (Berkelman and Lagarias, 1986). Zn^{2+}-induced luminescence from anti-phytochrome antibody–responsive polypeptides was visualized with a Bioimage analyzer (FMBIO-II; Hitachi Software Engineering Co., Kanagawa, Japan).

Immunostaining of Cryosections

Cryosections (8 μm thick) were prepared from the dark-adapted Vallisneria leaves according to the methods of Hisada et al. (2000). As the primary antibodies, culture supernatants of hybridoma for anti-phytochrome monoclonal antibodies (Table 4) were used directly without dilution. After incubation with the primary antibody, the sections were treated with biotinylated anti-mouse IgG antibody and avidin-conjugated horseradish peroxidase for 30 min each according to the manufacturer's instructions (ABC kit; Vector Laboratories, Burlingame, CA). After incubating the sections with biotinyl tyramide (TSA amplification kit; DuPont–New England Nuclear) for 5 min, the immunosignals were visualized by an additional treatment with avidin-conjugated fluorescein (Vector Laboratories). The sections were examined by optical microscopy (AX70; Olympus) as described by Hisada et al. (2000).

Staining of Actin Filaments

Actin filaments along the outer periclinal walls of epidermal cells were visualized by staining with fluorescently labeled phalloidin (Alexa Fluor 488 phalloidin; Molecular Probes, Eugene, OR) as described by Dong et al. (1998) with minor modifications.

Upon request, all novel materials described in this article will be made available in a timely manner for noncommercial research purposes.

ACKNOWLEDGMENTS

This paper is dedicated to the late Prof. emeritus Noburo Kamiya of Osaka University, who had made a great contribution to plant cell biology. The authors are deeply indebted to Akira Nagatani (Kyoto University) for permission to use purified monoclonal antibodies, to James L. Weller (University of Tasmania) for critical reading of the manuscript, and to Shigeru Uchiyama (Hamamatsu Photonics) for kind cooperation in improving the software. Thanks are due as well to Nami Sakurai (Osaka University) for excellent staining of actin filaments and to Michinari Kouzuma (Hitachi Ltd., Instrument Division) for collaboration in the early stages of this study. This work was supported in part by Grant B2023 from the Hitachi Advanced Research

Laboratory and by a grant from the Program for the Promotion of Basic Research Activities for Innovative Biosciences to M.F.

Received August 18, 2002; accepted November 6, 2002.

REFERENCES

Awata, J., Saitoh, K., Shimada, K., Kashiyama, T., and Yamamoto, K. (2001). Effects of Ca^{2+} and calmodulin on the motile activity of characean myosin in vitro. Plant Cell Physiol. **42,** 828–834.

Berkelman, T.R., and Lagarias, J.C. (1986). Visualization of bilin-linked peptides and proteins in polyacrylamide gels. Anal. Biochem. **156,** 194–201.

Bischoff, F., Millar, A.J., Kay, S.A., and Furuya, M. (1997). Phytochrome-induced intercellular signalling activates cab::luciferase gene expression. Plant J. **12,** 839–849.

Britz, S.J. (1979). Chloroplast and nuclear migration. In Encyclopedia of Plant Physiology, New Series, Vol. 7, W. Haupt and M.E. Feinleib, eds (Berlin: Springer-Verlag), pp. 170–205.

Dong, X.-J., Nagai, R., and Takagi, S. (1998). Microfilaments anchor chloroplasts along the outer periclinal wall in *Vallisneria* epidermal cells through cooperation of Pfr and photosynthesis. Plant Cell Physiol. **39,** 1299–1306.

Dong, X.-J., Takagi, S., and Nagai, R. (1995). Regulation of the orientation movement of chloroplasts in epidermal cells of *Vallisneria*: Cooperation of phytochrome with photosynthetic pigment under low-fluence-rate light. Planta **197,** 257–263.

Ermolayeva, E., Hohmeyer, H., Johannes, E., and Sanders, D. (1996). Calcium-dependent membrane depolarisation activated by phytochrome in the moss *Physcomitrella patens*. Planta **199,** 352–358.

Fankhauser, C., Yeh, K.-C., Lagarias, J.C., Zhang, H., Elich, T.D., and Chory, J. (1999). PKS1, a substrate phosphorylated by phytochrome that modulates light signaling in *Arabidopsis*. Science **284,** 1539–1541.

Furuya, M. (1993). Phytochromes: Their molecular species, gene families, and functions. Annu. Rev. Plant Physiol. Plant Mol. Biol. **44,** 617–645.

Furuya, M., and Inoue, Y. (1994). Instrumentation in photomorphogenesis research. In Photomorphogenesis in Plants, R.E. Kendrick and G.H.M. Kronenburg, eds (Dordrecht, The Netherlands: Kluwer Academic Publishing), pp. 29–40.

Gilroy, S., Fricker, M.D., Read, N.D., and Trewavas, A.J. (1991). Role of calcium in signal transduction of *Commelina* guard cells. Plant Cell **3,** 333–344.

Gunning, B.E.S. (1982). The cytokinetic apparatus: Its development and spatial regulation. In The Cytoskeleton in Plant Growth and Development, C.W. Lloyd, ed (London: Academic Press), pp. 229–292.

Haupt, W., Mörtel, G., and Winkelnkemper, I. (1969). Demonstration of different dichroic orientation of phytochrome Pr and Pfr. Planta **88,** 183–186.

Hisada, A., Hanzawa, H., Weller, J.L., Nagatani, A., Reid, J.B., and Furuya, M. (2000). Light-induced nuclear translocation of endogenous pea phytochrome A visualized by immunocytochemical procedures. Plant Cell **12,** 1063–1078.

Izutani, Y., Takagi, S., and Nagai, R. (1990). Orientation movements of chloroplasts in *Vallisneria* epidermal cells: Different effects of light at low- and high-fluence rate. Photochem. Photobiol. **51,** 105–111.

Jaffe, M.J. (1968). Phytochrome-mediated bioelectric potentials in mung bean seedlings. Science **162,** 1016–1017.

Kagawa, T., and Wada, M. (1994). Brief irradiation with red or blue light induces orientational movement of chloroplasts in dark-adapted prothallial cells of the fern *Adiantum*. J. Plant Res. **107,** 389–398.

Kagawa, T., and Wada, M. (2000). Blue light-induced chloroplast relocation in *Arabidopsis thaliana* as analyzed by microbeam irradiation. Plant Cell Physiol. **41,** 84–93.

Kikuyama, M., and Tazawa, M. (1983). Transient increase of intracellular Ca^{2+} during excitation of tonoplast-free *Chara* cells. Protoplasma **117,** 62–67.

Kircher, S., Kozma-Bognar, L., Kim, L., Adam, E., Harter, K., Schäfer, E., and Nagy, F. (1999). Light quality-dependent nuclear import of the plant photoreceptors phytochrome A and B. Plant Cell **11,** 1445–1456.

Kusumi, A., and Sako, Y. (1996). Cell surface organization by the membrane skeleton. Curr. Opin. Cell Biol. **8,** 566–574.

Lewis, B.D., Karlin-Neumann, G., Davis, R.W., and Spalding, E.P. (1997). Ca^{2+}-activated anion channels and membrane depolarizations induced by blue light and cold in *Arabidopsis* seedlings. Plant Physiol. **114,** 1327–1334.

López-Juez, E., Nagatani, A., Tomizawa, K.-I., Deak, M., Kern, R., Kendrick, R.E., and Furuya, M. (1992). The cucumber long hypocotyl mutant lacks a light-stable PHYB-like phytochrome. Plant Cell **4,** 241–251.

Mineyuki, Y., Takagi, M., and Furuya, M. (1984). Changes in organelle movement in the nuclear region during the cell cycle of *Adiantum* protonema. Plant Cell Physiol. **25,** 297–308.

Mineyuki, Y., Yamada, M., Takagi, M., Wada, M., and Furuya, M. (1983). A digital image processing technique for the analysis of particle movements: Its application to organelle movements during mitosis in *Adiantum* protonemata. Plant Cell Physiol. **24,** 225–234.

Nagai, R. (1993). Regulation of intracellular movements in plant cells by environmental stimuli. Int. Rev. Cytol. **145,** 251–310.

Nagatani, A., Chory, J., and Furuya, M. (1991). Phytochrome B is not detectable in the *hy3* mutant of *Arabidopsis*, which is deficient in responding to end-of-day far-red light treatments. Plant Cell Physiol. **32,** 1119–1122.

Neff, M.M., Fankhauser, C., and Chory, J. (2000). Light: An indicator of time and place. Genes Dev. **14,** 257–271.

Newman, I.A. (1981). Rapid electric responses of oats to phytochrome show membrane processes unrelated to pelletability. Plant Physiol. **68,** 1494–1499.

Nick, P. (1998). Signaling to the microtubular cytoskeleton in plants. Int. Rev. Cytol. **184,** 33–80.

Nick, P., Ehmann, B., Furuya, M., and Schäfer, E. (1993). Cell communication, stochastic cell responses, and anthocyanin pattern in mustard cotyledon. Plant Cell **5,** 541–552.

Nishizaki, Y. (1988). Blue light pulse-induced transient changes of electric potential and turgor pressure in the motor cells of *Phaseolus vulgaris* L. Plant Cell Physiol. **29,** 1041–1046.

Oelze-Karow, H., and Mohr, H. (1973). Quantitative correlation between spectrophotometric phytochrome assay and physiological response. Photochem. Photobiol. **18,** 319–330.

Quail, P.H. (1983). Rapid action of phytochrome in photomorphogenesis. In Encyclopedia of Plant Physiology, New Series, Vol. 16A, W. Shropshire, Jr., and H. Mohr, eds (Berlin: Springer-Verlag), pp. 178–212.

Quail, P.H., Boylan, M.T., Parks, B.M., Short, T.W., Xu, Y., and

Wagner, D. (1995). Phytochromes: Photosensory perception and signal transduction. Science **268,** 675–680.

Quail, P.H., Marmé, D., and Schäfer, E. (1973). Particle-bound phytochrome from maize and pumpkin. Nat. New Biol. **245,** 189–191.

Racusen, R.H. (1976). Phytochrome control of electrical potentials and intercellular coupling in oat-coleoptile tissue. Planta **132,** 25–29.

Schönbohm, E. (1972). Experiments on the mechanism of chloroplast movement in light oriented chloroplast arrangement. Acta Protozool. **11,** 211–223.

Schütz, I., and Furuya, M. (2001). Evidence for type II phytochrome-induced rapid signalling leading to *cab*::*luciferase* gene expression in tobacco cotyledons. Planta **212,** 759–764.

Shinomura, T., Nagatani, A., Hanzawa, H., Kubota, M., Watanabe, M., and Furuya, M. (1996). Action spectra for phytochrome A- and B-specific photoinduction of seed germination in *Arabidopsis thaliana*. Proc. Natl. Acad. Sci. USA **93,** 8129–8133.

Shinomura, T., Uchida, K., and Furuya, M. (2000). Elementary processes of photoperception by phytochrome A for high irradiance response of hypocotyl elongation in *Arabidopsis thaliana*. Plant Physiol. **122,** 147–156.

Staiger, C.J. (2000). Signaling to the actin cytoskeleton in plants. Annu. Rev. Plant Physiol. Plant Mol. Biol. **51,** 257–288.

Takagi, S., and Nagai, R. (1983). Regulation of cytoplasmic streaming in *Vallisneria* mesophyll cells. J. Cell Sci. **62,** 385–405.

Takagi, S., and Nagai, R. (1985). Light-controlled cytoplasmic streaming in *Vallisneria* mesophyll cells. Plant Cell Physiol. **26,** 941–951.

Takagi, S., Yamamoto, K.T., Furuya, M., and Nagai, R. (1990). Cooperative regulation of cytoplasmic streaming and Ca^{2+} fluxes by Pfr and photosynthesis in *Vallisneria* mesophyll cells. Plant Physiol. **94,** 1702–1708.

Tazawa, M., and Shimmen, T. (1987). Cell motility and ionic relations in characean cells as revealed by internal perfusion and cell models. Int. Rev. Cytol. **109,** 259–312.

Wada, M., Grolig, F., and Haupt, W. (1993). Light-oriented chloroplast positioning: Contribution to progress in photobiology. J. Photochem. Photobiol. B Biol. **17,** 3–25.

Williamson, R.E., and Ashley, C.C. (1982). Free Ca^{2+} and cytoplasmic streaming in the alga *Chara*. Nature **269,** 647–651.

Yamaguchi, Y., and Nagai, R. (1981). Motile apparatus in *Vallisneria* leaf cells. I. Organization of microfilaments. J. Cell Sci. **48,** 193–205.

Yokota, E., Muto, S., and Shimmen, T. (1999). Inhibitory regulation of higher-plant myosin by Ca^{2+} ions. Plant Physiol. **119,** 231–239.

Yokota, E., Muto, S., and Shimmen, T. (2000). Ca^{2+}-calmodulin suppresses the F-actin-binding activity of a 135-kDa actin-bundling protein isolated from lily pollen tubes. Plant Physiol. **123,** 645–654.